Perspectives of the Smart Cu-Iodine Coordination Polymers: A Portage to the World of New Nanomaterials and Composites

Javier Conesa Egea,[a,b]* Félix Zamora[a,b,c]* and Pilar Amo-Ochoa[a,c]*

[a]Departamento de Química Inorgánica, Universidad Autónoma de Madrid, 28049 Madrid, Spain. E-mail: pilar.amo@uam.es

[b] Condensed Matter Physics Center (IFIMAC), Universidad Autónoma de Madrid, 28049 Madrid, Spain

[c]Instituto de Investigación Avanzada en Ciencias Químicas de la UAM. Madrid. Spain

Abstract

This work is focused on the chemistry and physical properties of a particular family of coordination polymers (CPs) based on copper-iodine chains bearing functionalized pyridine, pyrimidine and pyrazine ligands. Although this family of compounds has been well-described, most of the studies have been focused on structural characterization and optical properties in bulk scale while works rationalizing their stimuli-responsive behavior and the role of these materials at the nanoscale are being reported very rencently. This article describes the first works in these fields and the perspectives that nanoscaled CPs based on Cu(I)-halide will have in the near future. Thus, the aim of this review is to present the new perspectives that are opening for these materials by deepening in their behavior, considering theoretical calculations, size-dependent properties or their combination with other components to form new hybrid materials. The combination of all these aspects will allow the discovery of interesting materials useful in sensing, nanochips or packaging, among other uses.

Keywords: Smart materials, nanomaterials; smart composites; stimuli-response materials; coordination polymers.

1. Introduction

Coordination Polymers (CPs) are compounds formed by the linkage of metal entities and organic or inorganic ligands. In this type of compounds, the proper selection of the building blocks allows the synthesis of materials with different architectures and physico-chemical properties, from molecular recognition to magnetic, electrical and/or optical materials including porous materials, namely metal-organic frameworks, MOFs[1-6]. Only with copper(I) as a metal center, there are thousands of CPs and discrete cluster complexes with different structures and properties. A large sub-family are those formed by Cu(I) halide chains (Cu(I)-X, where X is a halide) with general formula $[CuX(L)]_n$ (L= organic ligands) (Figure 1) which were discovered for more than a century [7], and in 1970s presented a vertiginous increase in their synthesis and properties studies, thanks to the advances in the single crystal X-ray diffraction techniques [8-35].

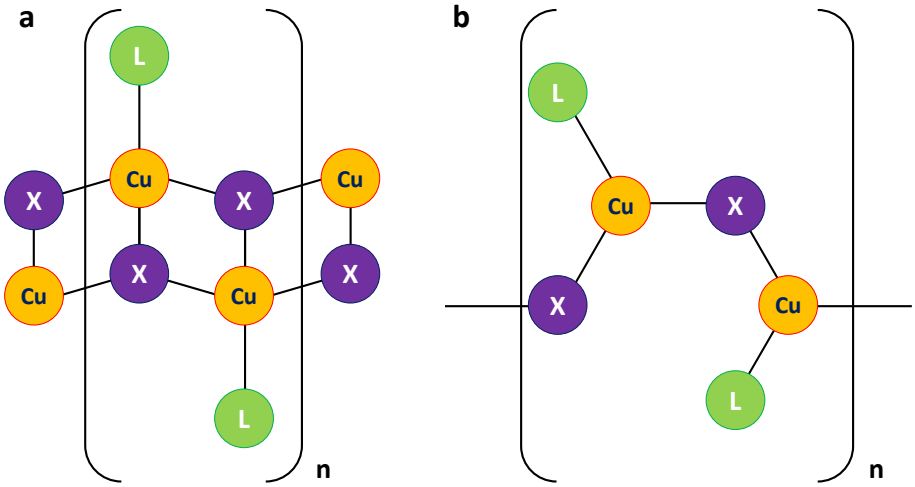

Figure 1. Scheme of the most important motifs adopted by the Cu(I)-X (where X is a halide or pseudohalide and L is and organic ligand) coordination polymers.

The studies of this type of compounds have been focused on two main lines: Firstly, their ability to form interesting structures from the point of view of crystal engineering [36-45]. Secondly, their interesting luminescent properties that have allowed obtaining new useful materials for sensing or optoelectronic applications [22, 46, 47]. At present, many Cu(I)-I clusters have been described as possible candidates to be OLED components, due to their easy processability, solubility and electroluminescent properties [48, 49]. As for Cu(I)-I coordination polymers, there is a number of examples which show structural changes affecting their physical properties, when exposed to certain vapors [19, 21, 50, 51]. Therefore, these materials have been suggested for device fabrication for the detection of gases.

The goal of this article is not making a full revision on Cu(I) halide CPs , because there are nice reviews [28, 52, 53] describing the synthesis, structure and properties of this family of compounds, but focusing on new synthetic approaches for their preparation as nanomaterials and the possibilities to form hybrid nanomaterials towards nanodevices fabrication and applications in other technological fields. Today, Cu(I) halide CPs represent a prominent family of materials with interesting luminescent [54] and electrical [55, 56] properties that enable them to have technological applications in different industrial fields such as catalysis [57, 58], food [59-61], packaging or aerospace [62, 63]. However, only very recently deep studies focusing on their mechanism of action are starting to be described, allowing the understanding of some unclear behaviors [19, 64-66].

Currently, Cu(I)-I CPs are starting to be used for the fabrication of new hybrid materials with organic polymers such as poly(methyl methacrylate) (PMMA), to modify their physical properties, providing them , for instance, fluorescence and/or semiconductivity at the time that retaining the mechanical properties of the organic matrix. This will probably allow the fabrication of novel optical fibre, farm plastic films or organic fluorescent glass [67]. So far, the vast majority of articles published on this type of compounds do not discriminate the study of their properties in function of the material size. Therefore, the nanoprocessing of these materials will surely open new perspectives in nanotechnological applications.

In view of these new perspectives, this article is divided into three sections: *i*) in the first one it is outlined the stimuli-responsive mechanisms of action of which Cu(I)-I chain based CPs have been objected to study; *ii*) Then, a description of the methods used to nanoprocess these CPs is revised; and finally *iii*) it is disclosed one of the applications that derive from this nanoprocessing, meaning the implement of Cu(I)-I based nanoparticles into organic matrices to form composite materials. These latter aspects are still in their infancy, but if they are united, the creation of new nanomaterials will be possible and, therefore, we will be able to open up the frontiers of the application of these compounds.

2. Studies focused on the stimuli-response and conductive mechanisms of action of Cu(I)-I double chains.

The combination of coordination bonds with short copper-copper distances and a very good overlapping between the orbitals of copper and iodine as a consequence of their structural disposition and the big size of the iodine, produce flexible bonds, that make these chains behave as elastic springs-like structures acting as sensors against different types of stimuli such as temperature, pressure or the presence of certain solvents. These stimuli slightly modify the distances and angles of their structures causing a response in their physical properties *i.e.* emission and/or conductivity.

2.1. Temperature-dependent properties

Cu(I)-I double chains are especially sensitive to temperature changes, since the usual structural contraction that compounds suffer when temperature decreases, this originates a shortening of Cu···Cu and Cu-I distances, typically allowing a better interaction between these atoms.

The shortening of Cu···Cu distances, generating interactions known as "cuprophilic", is known to be the main reason for luminescence thermochromism. Cuprophilicity has been studied for years [52, 68, 69] and its effect on the luminescent properties of Cu(I) compounds has been evaluated both in clusters and chain-based CPs.

The first example of a luminescent thermochromic compound based on a copper(I) iodide cluster was described by Hardt and co-workers in 1977 [70]. In this case, $[CuI(py)]_4$ (where *py* is pyridine) displayed a shift on its emission from yellow (600 nm) to blue (450 nm) when lowering the temperature from 298 K to 77 K. Since that discovery, many other Cu(I)-I clusters with substituted pyridines as terminal ligands have been synthesized and studied [49, 52, 71]. In all cases, luminescence at room temperature is associated with a combination of a halide-to-metal charge transfer (^{3}XMCT) and a cluster-centered $3d^{10} \rightarrow 3d^9 4(s,p)^1$ transition (^{3}CC), whereas at low temperatures a higher energy transition associated to a halide-to-ligand charge transfer (^{3}XLCT) arises.

This observation has also been verified for CPs where $(CuI)_x$ clusters are part of the structural moiety of the compound, with the same findings [9, 72]. In some cases, the thermochromic behavior of these clusters can be combined with the properties of another feature of the compound, like another metal structure. This is the case of the 3-dimensional metal-organic framework (MOF) $[(Cu^I_4I_4)_3(Cu^I_6)_2(3\text{-ptt})_{12}]_n \cdot 24n\text{DEF} \cdot 12nH_2O$ (3-ptt = 5-(3-pyridyl)-1*H*-1,2,4-triazole-3-thiolate; DEF = diethylformamide), described by Hong and co-workers [73]. In this CP, the thermochromic behavior displayed by the $[Cu_4I_4]$ cluster coexists with the near infrared (NIR) emission of the $[Cu_6S_6]$ clusters, creating a compound with an extremely rare dual emission which exists because the electronic states involving each metal cluster do not interfere. Thus, at room temperature, this compound displays only a NIR emission corresponding to that of the $[Cu_6S_6]$ cluster, whereas at low temperatures this NIR band shifts to lower energies and a new intense emission centered at 590 nm shows up (Figure 2).

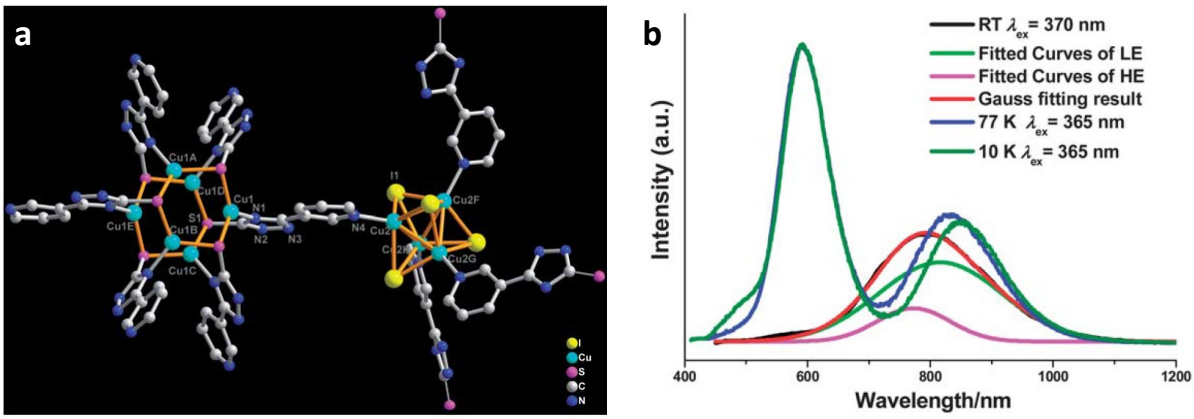

Figure 2. (a) Assymetric unit of $[(Cu^{I}_4I_4)_3(Cu^{I}_6)_2(3\text{-ptt})_{12}]_n \cdot 24nDEF \cdot 12nH_2O$; hydrogen atoms are omitted for clarity. (b) Experimental emission spectra of $[(Cu^{I}_4I_4)_3(Cu^{I}_6)_2(3\text{-ptt})_{12}]_n \cdot 24nDEF \cdot 12nH_2O$ at room temperature (black) and low temperatures (blue and dark green), and theoretical fits of the room temperature spectrum. Adapted from reference [73]; copyright 2013 Royal Society of Chemistry.

The thermoluminescent properties of CPs based on Cu(I)-I double *zig-zag* chains follow the similar principles than those of cluster-based compounds, since Cu···Cu distances, or at least half of them, also tend to be closely similar to 2.80 Å, twice the van der Waals radius of Cu(I), and therefore they display the same ^{3}XMCT and ^{3}CC transitions at room temperature, although the transition at low temperatures implies a charge transfer between the metal-halide skeleton and the ligand, namely ^{3}(M+X)LCT. Still, depending on the terminal ligands of the Cu(I)-I double chains, the thermochromism displayed by each CP may drastically vary (Table 1). For example, one-dimensional CPs with the formula $[Cu(L)I]_n$, with L being methyl isonicotinate (MeIN) or methyl 2-aminoisonicotinate (NH_2-MeIN), display very different thermochromic behavior at temperatures between 80 and 300 K. Thus, $[Cu(MeIN)I]_n$ shows a bright orange luminescence at room temperature, with λ_{em} = 614 nm; while when the temperature decreases, this emission is gradually weakened and, below 120 K, the emission band splits into two peaks with λ_{em} centered at 593 and 642 nm. On the other hand, $[Cu(NH_2\text{-}MeIN)I]_n$ shows no appreciable luminescence at room temperature, but upon lowering the temperature starts to show luminescence with a band at 550 nm and a shoulder at 516 nm at enhances in intensity by decreasing the temperature 80 K (Figure 3) [74].

Table 1. Temperature-dependent emissive behavior data of some Cu(I)-I double-chain-based coordination polymers.

CP	Dimensionality	T (K)	λ_{em} (nm)	Cu-Cu distances (Å)	Reference
$[Cu_2I_2(pyz)]_n$	2D	300 80	560 606	2.805 (unpublished)	*[75, 76]*
$[Cu_2I_2(Apyz)]_n$	2D	300	630	2.715; 3.253	*[65]*

		80	566	2.660; 3.269*	
$[Cu_2I_2(2\text{-Clpyz})]_n$	2D	300 80	628 616	(Structure not available)	*[75]*
$[Cu_2I_2(2,3\text{-dmpyz})]_n$	2D	300	544	2.736	*[77]*
$[Cu_2I_2(2,5\text{-dmpyz})]_n$	2D	300	570	2.797	*[22]*
$[Cu(2,6\text{-dmpyz})I]_n$	1D	300	533	2.748	*[22]*
$[Cu(4,6\text{-dmpym})I]_n$	1D	300	512	2.986	*[22]*
$[Cu(3,5\text{-lut})I]_n$	1D	300	436	2.889; 3.051	*[22]*
$[Cu_2I_2(4,4'\text{-bpy})]_n$	2D	300 80	541 568	2.845 (unpublished)	*[78]*
$[Cu(MeIN)I]_n$	1D	300 200 80	614 597, 625 593, 642	2.751; 2.823 2.719; 2.764 2.698; 2.724*	*[64, 74]*
$[Cu(EtIN)I]_n$	1D	300	567	2.797; 2.813	*[64]*
$[Cu(NH_2\text{-MeIN})I]_n$	1D	300 80	550 (I~0) 550, 516	2.682; 3.514 2.627; 3.523*	*[74]*

Legend: py = pyridine; pym = pyrimidine; pyz = pyrazine; Apyz = aminopyrazine; dmpyz = dimethylpyrazine; lut = lutidine (dimethylpyridine); bpy = bipyridine; MeIN = methyl isonicotinate; EtIN = ethyl isonicotinate; NH_2-MeIN = methyl 2-aminoisonicotinate. *Structures resolved at 110 K.

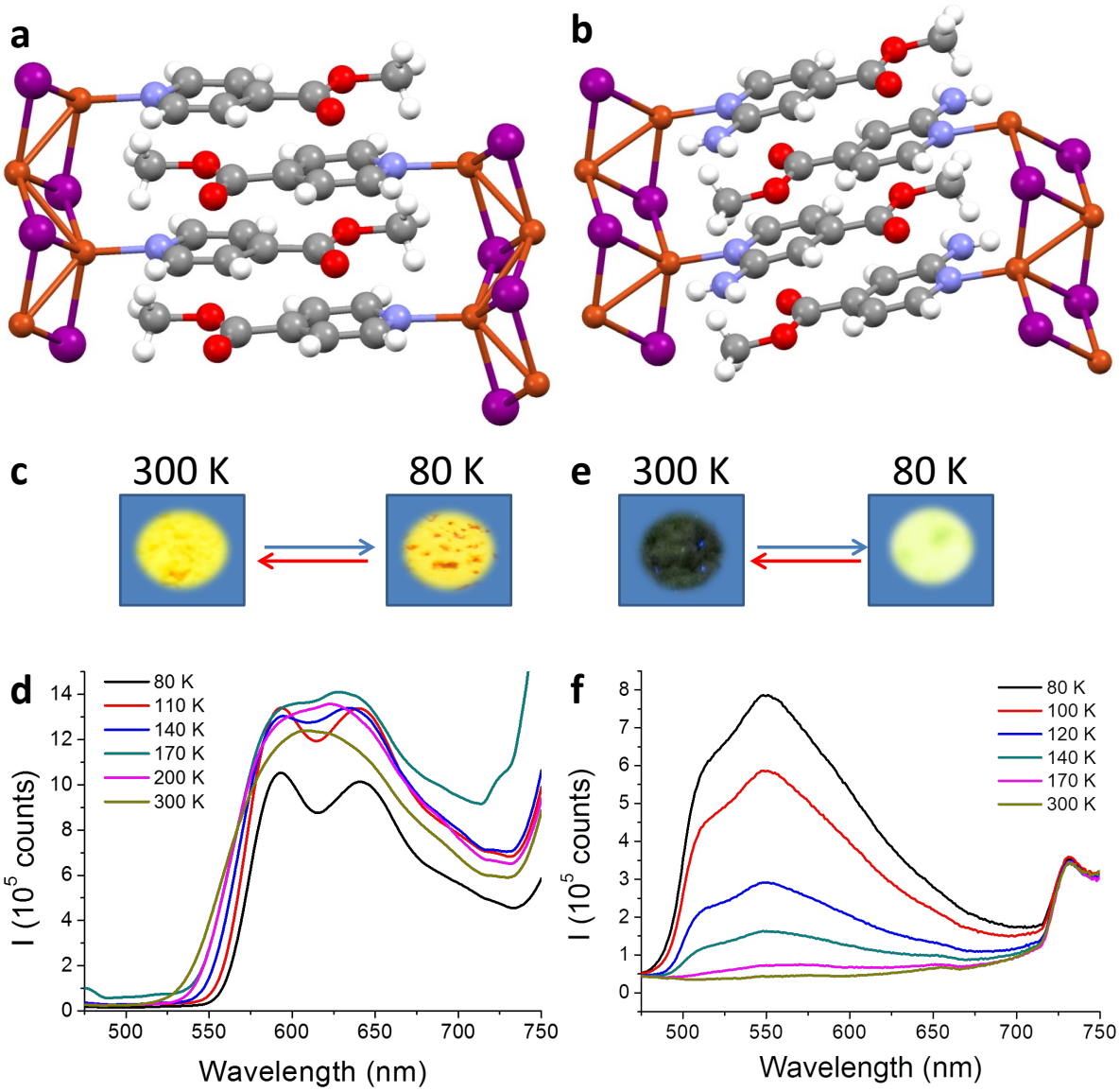

Figure 3. (a,b) Crystal structures of $[Cu(MeIN)I]_n$ (MeIN = methyl isonicotinate) (a) and $[Cu(NH_2\text{-}MeIN)I]_n$ (NH_2-MeIN = methyl 2-aminoisonicotinate) (b); Cu: orange; I: violet; C: gray; H: white; N; blue; O: red. (c) Representation showing the temperature-dependence behavior of $[Cu(MeIN)I]_n$ in the solid state under UV lamp excitation (λ_{exc} = 365 nm) at room temperature (left) and under liquid nitrogen (right). (d) Temperature-dependent luminescence spectra of $[Cu(MeIN)I]_n$. (e) Representation showing the thermochromic behaviour of $[Cu(NH_2\text{-}MeIN)I]_n$ in the solid state under UV lamp excitation (λ_{exc} = 365 nm) at room temperature (left) and under liquid nitrogen (right). (f) Temperature-dependent luminescence spectra of $[Cu(NH_2\text{-}MeIN)I]_n$. Adapted from reference [74] with permission, copyright 2018 Royal Society of Chemistry.

Apart from their luminescent properties, Cu(I)-I double chain-based CPs usually show semiconductive behavior, with electrical conductivities ranging from 10^{-9} to 10^{-3} Scm^{-1} [21, 79, 80]. Following this principle, when lowering the temperature, the electronic band gap will

grow and, therefore, the electrical conductivity of these CPs will decrease. This semiconductive behavior arises from the electronic delocalization along the Cu-I chains, favoured by the large size of the iodide ligands. If the asymmetry of the chain changes due to a phase transition provoked by a variation of temperature, some changes in the electrical conductivity will appear, and eventually this can encompass the presence of a hysteresis cycle (Figure 4). Thus, a one-dimensional CP reported by Hassanein *et al.* [64] showed a phase transition between 125 and 145 K, drastically changing its electrical conductivity in this temperature range, but keeping the semiconductive behavior (Figure 4).

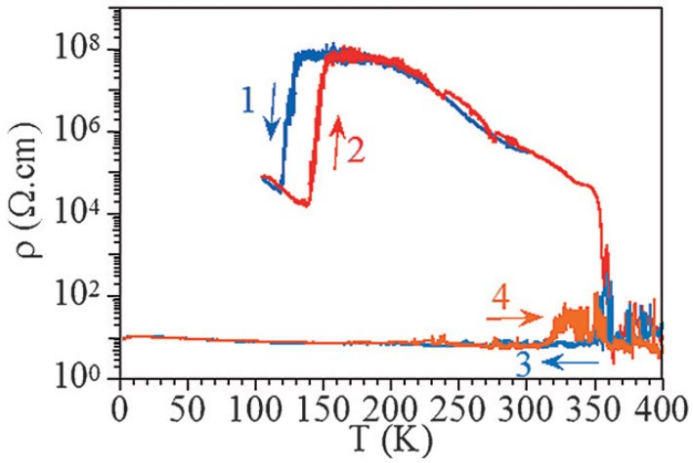

Figure 4. Variation of the electrical conductivity of $[Cu(MeIN)I]_n$ (MeIN= methyl isonicotinate) in four cooling and heating scans. Adapted from reference [64]; copyright 2015 Wiley-Verlag VCH.

According to their thermogravimetric analyses (TGA), Cu(I) based CPs and clusters usually start decomposing at about 100 ºC, so the study of temperature-dependent properties limiting the measurements below this value [64, 65, 74].

2.2. Pressure-dependent properties

Mechanical stresses can also affect Cu-I double chains, causing modifications in the Cu···Cu and Cu-I distances as well as temperature does. The effect of pressure on Cu(I)-I was first studied in 1977. Vogler and co-workers [81] coined the term "luminescence rigidochromism" referring to a change in the luminescence when the rigidity of the medium changed, *e. g.*, when freezing a solution containing the compound by applying pressure. Ford *et al.* [82] deepened in the study of the tetranuclear compound $[CuI(py)]_4$, (py = pyridine); in benzene solution at 1 bar, this compound presents an emission centered at 695 nm, corresponding to a ^{3}CC excited state. When freezing this solution, due to the action of pressure (at P > 72 MPa),

this emission band sharply shifts to 575 nm (Figure 5), close to that observed for the compound in the solid state (580 nm). This behavior was confirmed for solutions of this cluster-based complex in other solvents. However, unlike clusters, when a CP is dissolved either undergoes solvolysis or dissociates into its building blocks, giving rise, in both cases, to the CP cleaved and the formation of different species in solution; therefore, the studies of the pressure in solution are hampered and the pressure-dependent behavior of a CP must be carried out in the solid state.

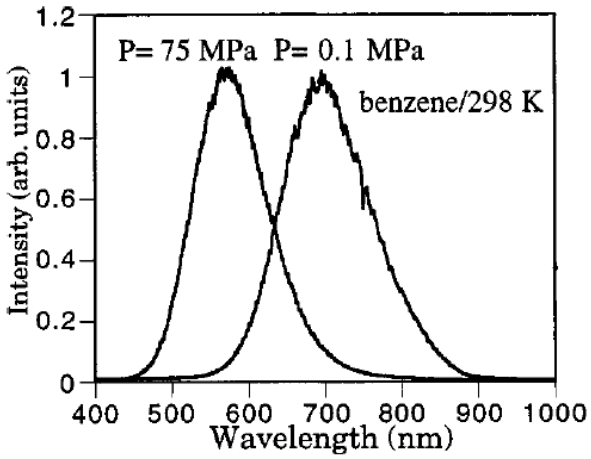

Figure 5. Emission spectra of $[CuI(py)]_4$ (py = pyridine) in benzene solution, at 1 bar and at 75 MPa. Adapted from reference [82], copyright 1997 American Chemical Society.

Initially, the most simple way to put one of these CPs through a mechanical stress is to grind it. Many studies carried out on Cu-I clusters and CPs show that, when they are ground, they suffer a loss of crystallinity or a phase transition which causes a sharp variation of their emission intensity and wavelength [23, 83].

Nevertheless, it has to be noticed that the pressure-depencence behavior is not showed for all the Cu-I double chain CPs, this is typically limited by the structural variations of the double Cu-I chains caused under pressure and the terminal ligands decorating the chains.

Another more complex experimental set-up to measure pressure-depencence consists of a diamond anvil cell allowing the use of ultra-high pressures with a suitable control of the measurement. This experimental set-up allows both the measurement of the changes in emission of the material at different pressures and its structural variations, therefore allowing establishing a comparison to rationalize the observed variations. Thus, González-Platas and co-workers [84] using this approach reported a 1D CP with 6-methylquinoline (6mq) as terminal ligand, namely $[Cu(6mq)I]_n$. This CP showed an emission centered at 550 nm at

ambient conditions, arising from a halide-to-ligand charge transfer excited state (^{3}XMCT); as pressure is raised above 800 MPa, and up to 6.45 GPa, three new emission bands centered at 515, 647 and 712 nm appear (Figure 6). The structural changes observed under pressure confirmed that Cu···Cu distances shrinked as pressure increased, from values of 2.796 and 3.466 Å at 1 bar to 2.683 and 2.932 Å at 6.45 GPa, in this case. Then, the appearance of these new bands was attributed to an enhancement of the cluster-centered transition (^{3}CC).

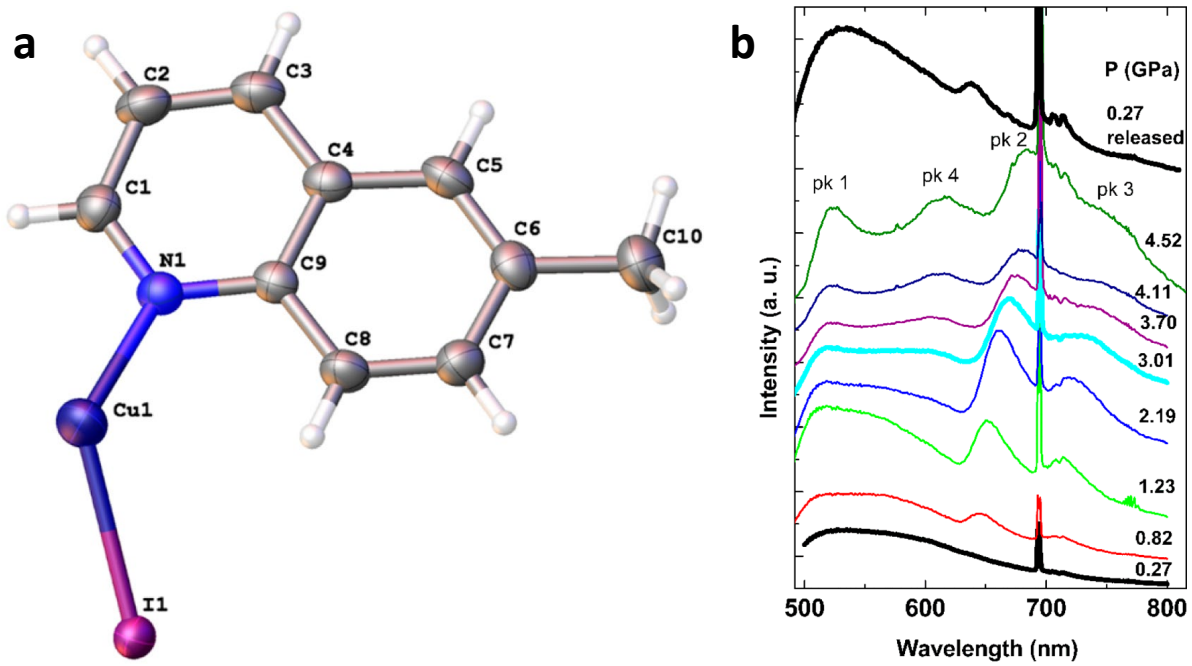

Figure 6. (a) Assymetric unit of the crystal structure of $[Cu(6mq)I]_n$ (6mq = 6-methylquinoline); C: gray, H: white, N: blue, Cu: indigo; I: purple. (b) Pressure-dependent emissive behavior of $[Cu(6mq)I]_n$; the sharp peak at 690 nm corresponds to the emission of a ruby used as pressure sensor. Adapted from reference [84], copyright 2016 American Chemical Society.

More recently, Amo-Ochoa and co-workers [65] reported a Cu-I double chain 2D CP which after compressing it with a mechanical press or in a diamond anvil cell, while the material remains crystalline its emission quenches due to a radical shortening of its Cu···Cu distances. A bad overlapping of the hybridized dz^2 orbitals of adjacent Cu atoms at high pressures is the cause of this loss of the emissive behavior (Figure 7). This fact has also been studied on similar CPs with one-dimensional structures [74].

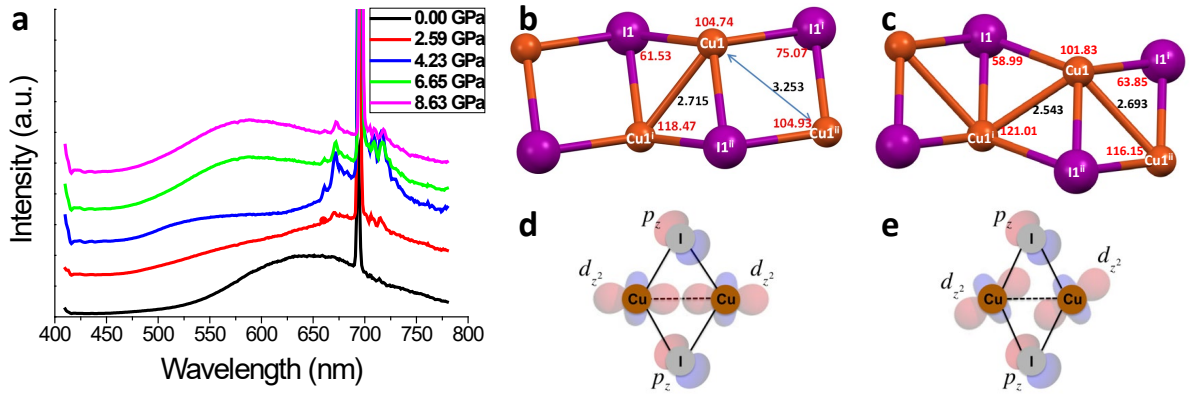

Figure 7. (a) Pressure dependence of the luminescence spectra of $[Cu_2I_2(Apyz)]_n$ (Apyz=2-aminopyrazine) (λ_{exc} = 375 nm). The sharp peak at 700 nm corresponds to ruby. (b, c) Representation of the Cu_2I_2 chain in $[Cu_2I_2(Apyz)]_n$ at ambient pressure (b) and at 8.35 GPa (c). (d, e) Theoretical representation of the copper d_z^2 orbitals and the iodine p_z orbitals in a Cu_2I_2 subunit of $[Cu_2I_2(Apyz)]_n$ at ambient pressure (d) and at 8.35 GPa (e). Adapted from reference [65]; copyright 2017 Wiley-Verlag VCH.

2.3. Response to vapors

As afore mentioned, Cu-I chain-based CPs can be also sensitive to chemical stimuli. Thus, for instance the presence of certain vapors of molecules can interact with these materials and produce a significant change in its physical properties *i.e.* emission and/or electrical conductivity. These vapor-to-solid interactions induce structural changes in the Cu-I chain CPs driven by the molecular recognition capabilities of certain terminal ligands. The interactions between the terminal ligands and the vapors can occur *via* π-π stacking, van der Waals forces and/or hydrogen bonds.

Since the discovery of $[Cu(py)I]_n$ (py = pyridine) (with n = 4 or ∞) [85, 86], many Cu(I)-I based CPs and clusters have been studied, but it was not until 1998 when Ford et al. [50] found out the first example of these compounds which showed a vapochromic behavior. $[Cu(4\text{-pic})I]_\infty$ (4-pic = 4-methylpyridine, or 4-pycoline) suffered a reversible transformation from its polymeric staircase motif into a four-member cluster, $[Cu(4\text{-pic})I]_4$, when exposed to toluene, both in liquid or vapor phase. On the contrary, when exposing $[Cu(4\text{-pic})I]_4$ to pentane, it reverted to the polymeric form $[Cu(4\text{-pic})I]_\infty$. This induced an evident change in the luminescent properties of the compound (Figure 8).

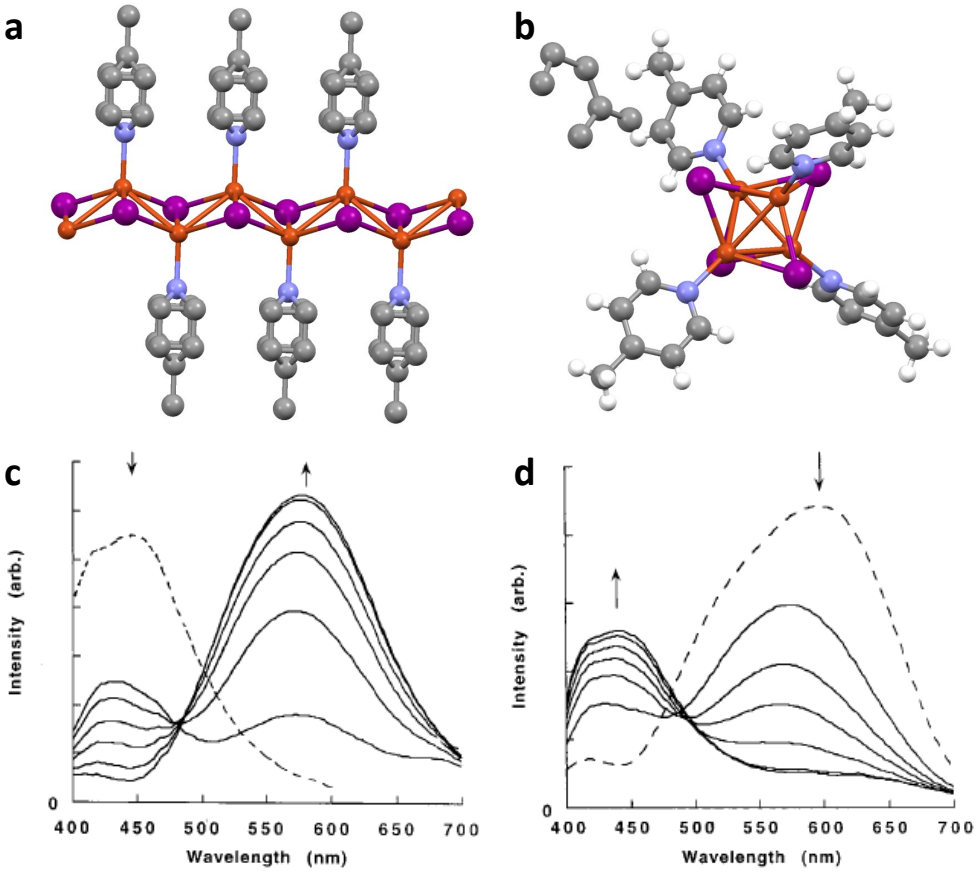

Figure 8. Crystal structures of $[Cu(4\text{-pic})I]_\infty$ (4-pic = 4-methylpyridine) (a) and $[Cu(4\text{-pic})I]_4$·Toluene (b). (c) Variation of the luminescence spectrum of $[Cu(4\text{-pic})I]_\infty$ as it transforms into $[Cu(4\text{-pic})I]_4$ in the presence of toluene. (d) Variation of the luminescence spectrum of $[Cu(4\text{-pic})I]_4$ as it transforms into $[Cu(4\text{-pic})I]_\infty$ in the presence of *n*-pentane. The shapes of the aromatic rings in (a) are due to a 50% delocalization for their orientation. (c, d) Adapted from reference [51]; copyright 2000 American Chemical Society.

This study has been extended to many other compounds since then. In 2000, Ford et al. [51] extended their studies to the similar compounds $[Cu(3\text{-pic})I]_\infty$ and $[Cu(3\text{-pic})I]_4$ (3-pic = 3-methylpyridine, or 3-pycoline), observing no response to gases.

More recently, Hassanein *et al.* [19, 21] reported a one-dimensional CP with 2-amino-5-nitropyridine (ANP) in its structure. Its high ability to establish hydrogen bonding interactions with some molecules proved it to be an excellent sensor for vapors of methanol, ethanol or, specially, acetic acid. When exposed to these molecules, the conductivity of this CP raised drastically, up to three orders of magnitude (Figure 9).

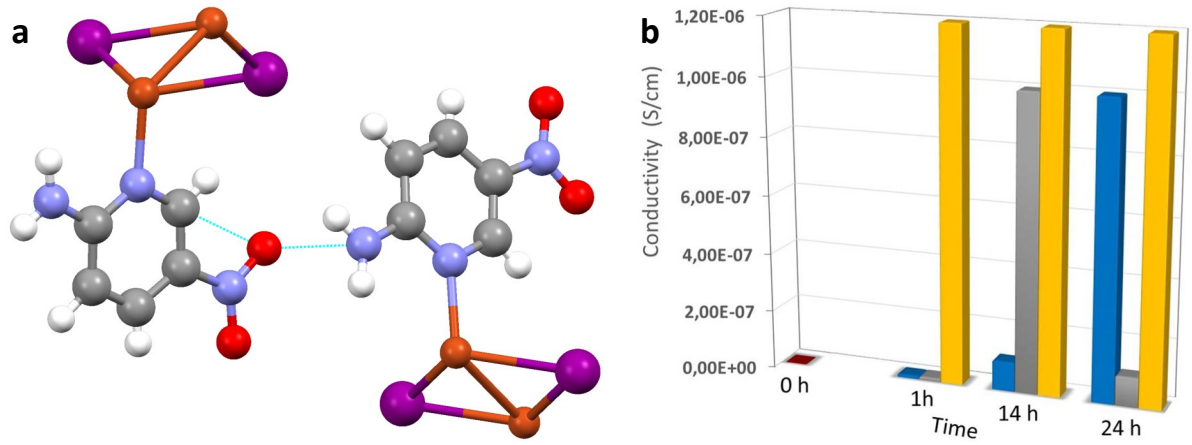

Figure 9. (a) Crystal structure of $[Cu(ANP)I]_n$ (ANP = 2-amino-5-nitropyridine) along the a axis. White: H; gray: C; blue: N; red: O; orange: Cu; purple: I. Dashed blue lines indicate hydrogen bonds. (b) Variation of the electrical conductivity of $[Cu(ANP)I]_n$: pristine (red), exposed to methanol (blue), ethanol (gray) or acetic acid (yellow). Adapted from reference [21]; copyright 2015 Royal Society of Chemistry.

3. Nanoprocessing of Cu(I)-I double chain CPs

Something began to change in 1959 when R. Feynman pronounced his famous phrase "there is plenty of room at the bottom" [87], culminating in 1980s when the physicists discovered the Scanning Tunneling Microscopy [88] and in the 1990s when we began to work in a usual way with the Atomic Force Microscopy [89], Then, science has entered a new dimension that has allowed extending the possibilities and options of materials.

Quantum effects can appear when a given material is reduced to the nanometer size, then switching their physical and/or chemical properties [90, 91]. For this reason, hundreds of new nanoscaled CPs have been described producing an emerging research field of interest for the new potential applications [3, 5, 83, 92-101]. In general, nanoscale production of CPs is based on two fundamental approaches: bottom-up and top-down techniques.

Bottom-up techniques are based on the adjustment of the reaction conditions to produce the materials directly with nanometer scale. One advantage of Cu(I)-I coordination polymers is that they are typically prepared by one-pot reactions based on the self-assembly of the selected building blocks. In this way, a CP usually precipitated and this process can be adjusted allowing to prepare materials with different sizes ranging from nano- to micro/milli-metric crystals. The structural characterization of the single-crystals is carried out using X-ray diffraction providing an atomic level of resolution while a simple approach for the

materials characterization at the nanoscale is based on the use of X-ray powder diffraction (XRPD) and its solution by comparison with the single-crystal data or using more complex solution approaches, e.g. *ab-initio*.

Additionally, the materials are generally characterized using other complementary spectroscopic techniques. In order to determine their morphology and size microscopic techniques are required. The most usual tools are electron microscopies, such as scanning electron microscopy (SEM) and transmission electron microscopy (TEM). Scanning Probe microscopies, such as atomic force microscopy (AFM) and scanning tunneling microscopy (STM) are becaming in many cases essential for a full characterization at the nanoscale. Additionally, the use of Dynamic Light Scattering (DLS) for CPs in suspensions provides suitable information about the size and is also useful for to stablish mechanism of material formation and growth.

The previous reviews found in the literature based on multinuclear and copper(I) coordination polymers with bridging halides have been focused on aspects related with their bulk synthesis and characterization, indeed they do not pay attention to the materials' size when describing aspects related to their physical properties, e.g. emission [28, 49, 102]. In general, these CPs are usually obtained by relatively simple synthetic routes, being most typical one the direct reaction between the selected building blocks: CuX (X = Cl, Br, I) and the organic ligand/s (L), under different reaction conditions: pressure, temperature, concentration and solvents under anaerobic conditions to avoid metal oxidation [103].

When working at moderate temperatures, due to their insolubility in the reaction medium, CPs precipitate quite quickly, and are therefore collected as solids with colors varying from yellow to red depending on the ligands used for their obtainment, and with material sizes ranging from microns to a few nanometres.

In all these cases the structural characterization of these compounds is based on a spectroscopic analysis by IR and an elemental analysis. By means of the use of a suitable method of crystallization, it is possible to obtain crystals appropriate for their characterization by single crystal X-ray diffraction and, in order to corroborate the structure with the obtained solid, the powder X-ray diffraction data of the sample are also taken. Finally, their properties are studied, obtaining results as afore mentioned. However, no studies on the size and morphology of the obtained solid are carried out, mistakenly assuming that it always shows micrometric sizes.

3.1. Methods for the nanoprocessing of Cu(I)-I based CPs

Recent articles show that direct syntheses of Cu-X double chains can immediately precipitate the CP in nanometric size. Therefore, special care must be taken in not mixing the results obtained from their properties, *i.e.* nanometric *versus* micrometric material size.

To date there are two fundamental approaches for nanoprocessing compounds based on the approaches of bottom-up and top-down synthesis. Bottom-up methodologies usually enclose on-surface (solid substrates) and interfacial syntheses (in liquid-liquid or liquid-air interfaces), whereas the most common top-down methods are micromechanical exfoliation and liquid-phase exfoliation [104].

In the case of Cu-X CPs, the general insolubility of this type of compounds allows the use of a top-down methodology based on sonication techniques in liquid phase (liquid phase exfoliation). This methodology gave its first fruits about 10 years ago, with interesting results like the ones obtained by Welte *et al.* for the 1D CP $[Cu(HIN)Br]_n$, where HIN is isonicotinic acid (Figure 10) [80] and for the mixed valence 2D CP $[Cu_2Br(IN)_2]_n$ (Figure 11) [105].

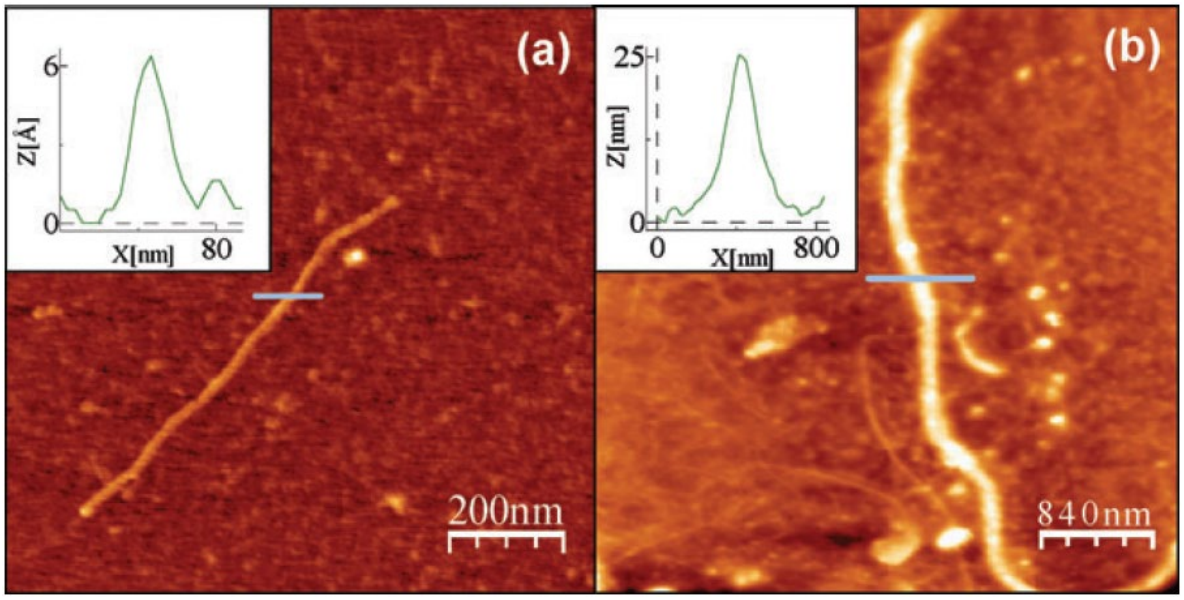

Figure 10. AFM topography images of $[CuBr(HIN)]_n$ (HIN = isonicotinic acid) nanowires deposited on polylisine treated mica (a) and gold (b) surfaces, with their respective height profiles across the blue lines on the upper-left corner. Reprinted from reference [80] with permission; copyright 2008 Royal Society of Chemistry.

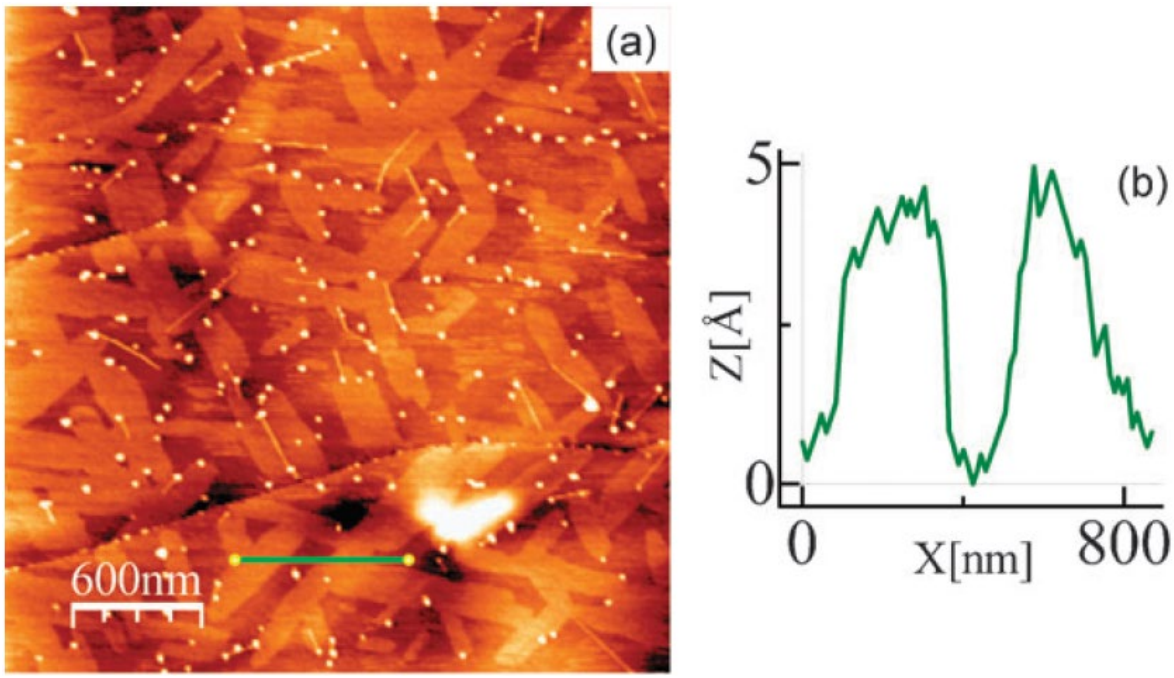

Figure 11. AFM topography image of $[Cu_2Br(IN)_2]_n$ (IN = isonicotinate) nanosheets deposited on highly oriented pyrolytic graphite (HOPG) (a), with its height profile across the line (b). Reprinted from reference [105] with permission; copyright 2010 Royal Society of Chemistry.

The second approach is based on the bottom-up method, although this methodology is truncated by the known insolubility of the CPs. In a preliminary work, the CP formation-solution reversibility process based on its solubility in specific solvents was successfully demonstrated in related MMX chains [56, 106-108]. One-dimensional mixed-valence CPs $[Pt_2(RCS_2)I]_n$ (where RCS_2^- is a dithiocarboxilate with R = *n*-pentyl) could be synthesized as nanowires with lengths of several microns and heights between 1.5 and 2.5 nm, corresponding to one to three MMX chains, by drop-casting of saturated solutions of their respective building blocks in THF over mica surfaces [106]. On the other hand, other MMX-based 1D CPs, namely $[Ru_2(EtCO_2)X]_n$ (where $EtCO_2^-$ is propionate and X^- is Br^- or I^-), the morphology of the obtained nanostructures depends on the bridging halide and the surface where they are deposited. $[Ru_2(EtCO_2)Br]_n$ structures deposited in mica starting from a solution of its building blocks in aqueous SDS show a typical nanofiber shape, whereas those deposited on highly oriented pyrolytic graphite (HOPG) show a helical structure derived from their interaction with the HOPG steps [107]. In the case of $[Ru_2(EtCO_2)I]_n$, sonication of ethanol solutions of its building blocks gave rise to different nanostructures depending on the subsequent incubation time at 20 ºC before depositing the solution over mica surfaces. Thus, immediately after the ultrasound treatment, nanostructures of this CP showed irregular shapes, proggressively evolving into well defined nanowires after 43 days of incubation [108].

More recently, Troyano *et al.* [109] carried out a solubility study on some CPs based on CuI and organosulphur ligands. It is well known that, when you dissolve a coordination polymer, it dissociates into its building blocks. Common solvents used to dissolve CPs are strongly coordinative (this is the case of DMF and DMSO), so the original structure of the CP cannot be recovered. However, when these Cu(I)-I based CPs are dissolved in acetonitrile, as the solvent evaporates they reorganize to form CP crystals. Therefore, when a drop of a saturated solution of these CPs is cast on a surface and allowed to evaporate, it leads to the formation of sub-micron structures with the same chemical composition and structure found for the analogous microcrystals, like the films obtained for $[CuI(TAA)]_n$ (TAA = thioacetamide) (Figure 12). Subsequent studies performed on other CuI CPs [64, 65, 110, 111] confirmed that most of these compounds show the same reversible behavior.

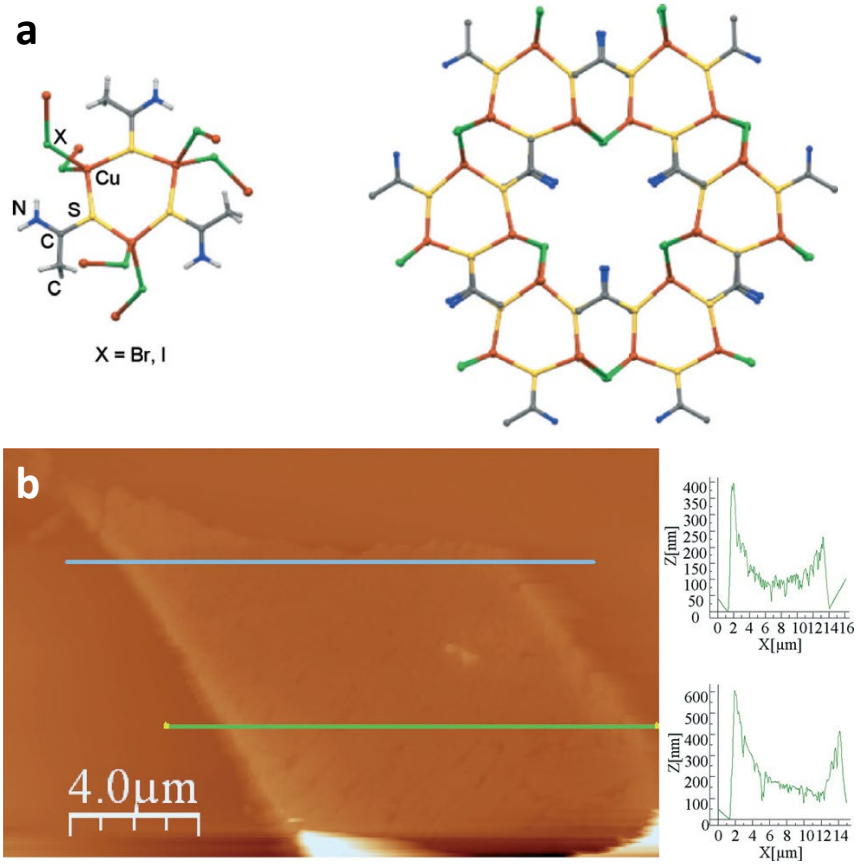

Figure 12. (a) Crystal structure of $[CuX(TAA)]_n$ (with X = Br or I), showing the basic Cu_6S_6 ring (left) and its connection with other rings *via* the halogen atoms to conform the 3-dimensional structure (right). (b) Topological AFM image of a $[CuI(TAA)]_n$ sheet formed by drop-casting of a saturated solution of the building blocks in acetonitrile, with its height profiles across the blue (up) and green lines (down). Adapted from reference [109]; copyright 2014 Royal Society of Chemistry.

This recent discovery is an important fact that has allowed the fruition of further studies on the preparation of Cu-X CP based nanostructures by bottom-up methods. In a similar way to what is explained above, the third and most recent approximation shows that the direct synthesis of these polymers (bottom-up) allows the *in situ* production of the polymer at the nanoscale, taking advantage of the insolubility of the CP in the reaction medium. Reversible CPs such as the ones described by Conesa-Egea *et al.* [65, 74] immediately crystallize into nanofibers or nanosheets when mixing the two building blocks (copper(I) iodide and the corresponding organic N-donor ligand). The first example to be described [65] consisted of a 2D CP with aminopyrazine as a bridging ligand between Cu(I)-I chains. When mixing solutions of copper(I) iodide in acetonitrile and aminopyrazine in distilled water, a yellow solid immediately precipitated. When this solid was deposited on SiO_2 by drop-casting and studied by SEM or AFM, it proved to be formed of films with lateral dimensions of microns and thicknesses from 50 to 300 nanometres. Later on [74], two more 1D CPs were prepared and deposited by the same method, obtaining long fibres with thicknesses of less than 15 nm (Figure 13).

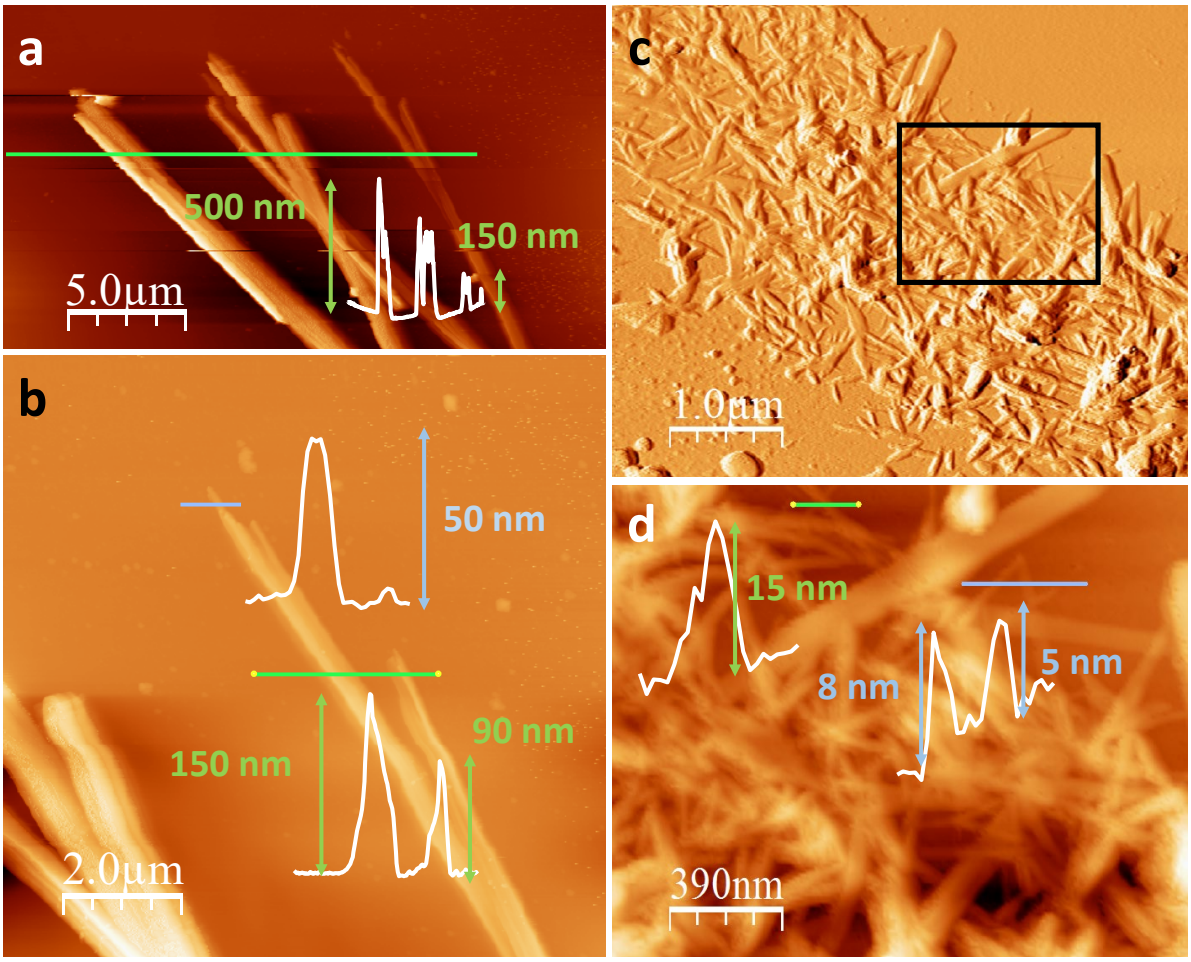

Figure 13. (a) AFM image of $[Cu(MeIN)I]_n$ (MeIN= methyl isonicotinate) nano- and sub-microfibers on SiO_2 prepared by drop casting, with their height profile across the green line. (b) A zoomed area of (a), with its height profiles across the blue and green lines. (c) AFM

image of $[Cu(NH_2\text{-}MeIN)I]_n$ (NH_2-MeIN= amino methyl isonicotinate) nanofibers on SiO_2 prepared by dip-coating. (d) A zoomed area of (c) (the black rectangle), with its height profiles across the green and blue lines. Reprinted from reference [74] with permission, copyright 2018 Royal Society of Chemistry.

As explained above, the properties of a material can significantly change with the material size when passing from the microscale to the nanoscale, due to quantum effects and the increase of its specific surface. In relation to this, it would be expected that, when the size of a CP is lowered, the splitting of the energy bands into discrete levels caused a change in its optical properties. In a first approximation, it was found that the thermochromism of $[Cu(MeIN)I]_n$ and $[Cu(NH_2\text{-}MeIN)I]_n$ was slightly different whether the spectra were measured in the crystalline form of these compounds (Figure 14) or in the nanometric powder (Figure 3d,f). Unfortunately, there are not many studies describing this kind of size-dependent behavior yet, so an effort must be made to go further with these findings.

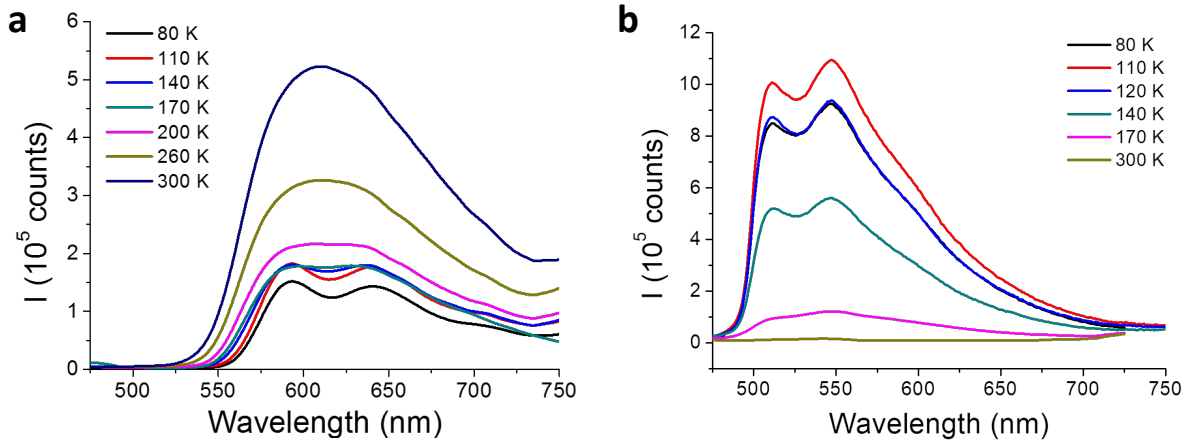

Figure 14. Temperature-dependent emission of $[Cu(MeIN)I]_n$ (a) and $[Cu(NH_2\text{-}MeIN)I]_n$ (b) as nanometric crystals. Adapted from reference [74] with permission, copyright 2018 Royal Society of Chemistry.

4. Fabrication of new hybrid materials using CPs based on Cu(I)-I chains.

The fabrication of composite materials including an organic matrix and a CP, also known as Mixed Matrix Membranes (MMM), is a field recently opened to research and, as explained above, success in the fabrication of these kind of composites will drastically broaden the industrial possibilities of these CPs.

The first example of a CP integrated in an organic matrix was described in 2015 by Rodenas *et al.* [112]. In this case, nanosheets of the two-dimensional MOF $[Cu(BDC)]_n$ (BDC = 1,4-benzenedicarboxilate, terephthalate) were implemented into a polyimide-based organic polymer in weight ratios between 2 and 12%. The adsorption properties of the MOF were retained when nanosheets were used as the dopant instead of micrometric crystals, due to the higher surface area that was exposed to the gas molecules and the homogeneous distribution of these nanosheets within the organic matrix.

Several attempts have been made to integrate MOFs into organic polymers such as polymethyl methacrylate (PMMA) [113, 114], obtaining free-standing MMMs (Figure 15) which retained the adsorption properties of the original MOF. Moreover, when combining other CPs with this organic matrix or others like polyvinylidene difluoride (PVDF), it is usual that both, the original properties of the CP and the mechanical properties of the organic matrix are retained in the MMM.

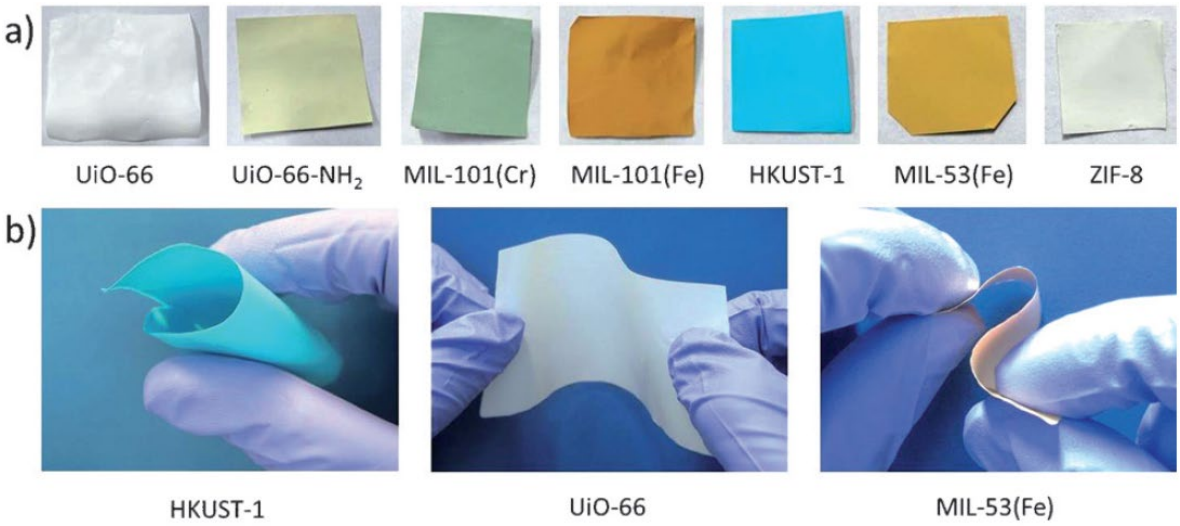

Figure 15. a) Free-standing MMMs (1 × 1 cm^2) produced from a variety of MOFs. b) Photographs demonstrating that large area MMMs containing HKUST-1, UiO-66, and MIL-53(Fe) (3 × 5 cm^2) are resilient to mechanical stress and can be easily handled. Reprinted from reference [113] with permission; copyright Wiley-Verlag VCH.

As far as Cu(I) based CPs are concerned, only two attempts to make MMMs has been reported so far. Troyano *et al.* [115] reported the formation of thin films based on two-dimensional Cu(I)-thiophenolate CPs with PVDF in a simple process where dissolved PVDF and the suspended CPs were mixed under ultrasound conditions; then the suspensions were deposited by drop-casting and, after evaporating the solvent at 85 ºC, homogeneous films were formed. The micrometric and nanometric thicknesses of the original CP crystals allowed the formation of thin composite films with thicknesses ranging from 35 to 75 µm (Figure 16). On the other hand, Conesa-Egea *et al.* [74] achieved the formation of thin

composite films with nanometric thicknesses by mixing nanocrystals of the 1D CP $[Cu(NH_2\text{-}MeIN)I]_n$ with PVDF by sonicating them, and depositing the resulting suspensions by dip-coating or spin-coating. In this case, we must remark the necessity of starting from nanocrystals of the CP; otherwise, the formation of MMMs with nanometric thickness would be impossible due to the big size of the crystals. The resulting thin films were free-standing and homogeneous, with thicknesses ranging from 25 to 60 nm, and retained the emissive behavior of the CP (Figure 17).

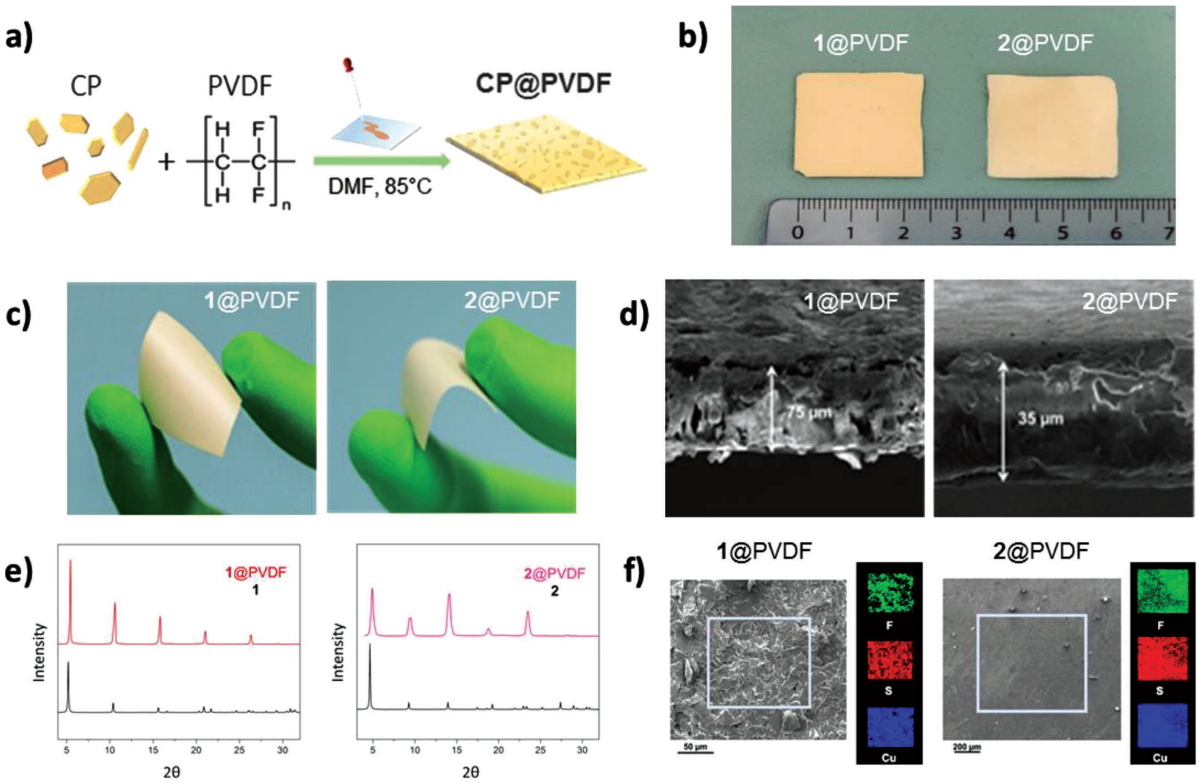

Figure 16. a) Schematic diagram of the fabrication of CP@PVDF composites via drop casting. b) Picture of as-prepared **1**@PVDF and **2**@PVDF thin films with 50% (wt%) of **1** and **2**, respectively. c) Pictures of **1**@PVDF and **2**@PVDF thin films showing their flexibility. d) Cross-section FESEM images of **1**@PVDF and **2**@PVDF thin films. e) XRPD patterns of **1**@PVDF (left) and **2**@PVDF (right) compared to the corresponding polycrystalline solids. f) SEM-EDS elemental mapping images of the outward facing surfaces of **1**@PVDF (left) and **2**@PVDF (right), showing the homogeneous distribution of fluorine (green), sulfur (red), and copper (blue). **1** = $[Cu(CT)]_n$, where CT = 4-carboxylthiophenolate; **2** = $[Cu(MCT)]_n$, where MCT = 4-methoxycarbonylthiophenolate. Reprinted with permission from reference [115], copyright 2018 Wiley-Verlag VCH.

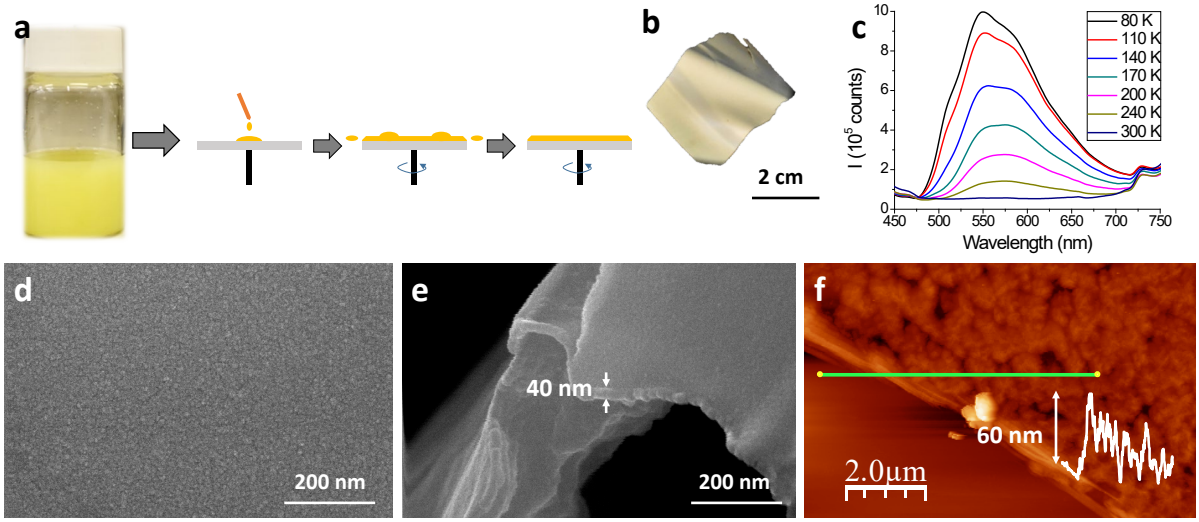

Figure 17. (a) Scheme of the spin-coating synthesis of the **[Cu(NH$_2$-MeIN)I]$_n$@PVDF** composite. (b) Photography of a 2 × 2 cm^2 **[Cu(NH$_2$-MeIN)I]$_n$@PVDF** thin-film. (c) Temperature-dependent emissive behavior of the **[Cu(NH$_2$-MeIN)I]$_n$@PVDF** film with 30% weight of [Cu(NH$_2$-MeIN)I]$_n$ (λ_{exc} = 375 nm). (d and e) SEM images of the **[Cu(NH$_2$-MeIN)I]$_n$@PVDF** thin-film with 4% weight of [Cu(NH$_2$-MeIN)I]$_n$. (f) AFM image of the **[Cu(NH$_2$-MeIN)I]$_n$@PVDF** thin film with 4% weight of [Cu(NH$_2$-MeIN)I]$_n$, and its height profile across the line. Adapted from reference [74] with permission, copyright 2018 Royal Society of Chemistry.

Based on all these experiments, more attempts to obtain composite films with nanometric thickness are being carried out at the moment. Starting from CP nanocrystals (with thicknesses of 10 nm or lower) and using other deposition methods such as dip-coating or spin-coating may be the key to achieve this goal.

5. Conclusions

Production and use of smart materials are subjects of high research and technological interest. Some CPs present the ability to reaccomodate their structure with slight changes in some angles and distances, with chemical and/or physical stimulus giving rise to changes in their physical properties.

Coordination polymers and complexes based on copper(I) halides and pseudohalides are a long-since known family of compounds, but they still attract the researchers interest due to their amazing optical properties. What is more, the easy way to synthesize them starting from

the building blocks (copper(I) salts and the corresponding ligands) makes their obtainment cheap and simply scalable to the industrial level.

This kind of compounds is dominated by Cu(I)-I clusters and chains, whose luminescent behavior is most remarkable thanks to the high polarizability of the iodide bridging ligands; this fact makes the Cu(I)-I chains behave like elastic springs which show slight modifications of the Cu···Cu and Cu-I distances and angles when exposed to external stimuli such as pressure, temperature or the presence of vapors. Thanks to this, these compounds present themselves as stimuli-responsive materials, featuring reversible changes in both the luminescence and the electrical conductivity (in the case of Cu(I)-I chain-based CPs) as these stimuli vary.

Despite the important characteristics displayed by CPs based on Cu(I)-I chains, their study has been limited to the structural level and to their luminescent properties as obtained. However, in the last four years an effort to produce nanostructures based on these compounds, thus providing a new kind of nanomaterials which preserve the properties of the compound, but adding them a size-dependent variation which, if slight, is important enough to force a deviation from the usual schemes followed so far when studying these CPs. This, added to the fact that their reversible solubility in some solvents and their insolubility in the reaction medium where they are obtained enormously facilitates the bottom-up formation of nanofibers or nanosheets based on them, may be the key for Cu(I)-I CPs to become the best substitutes of rare-earth based nanoparticles in the fabrication of luminescent nanodevices, since the higher availability of copper over lanthanides in the Earth crust will reduce the fabrication cost of these devices.

It is also worth mentioning that the recent data reported on the properties of the CPs based on Cu(I)-I chains at the nanoscale open new perspectives for their potential use but also they remark the importance of the analysis of the physico-chemical properties of these materials with the scale, *i.e.* macro *vs* nanoscale.

Last, but not least, the rising interest attracted by the combination of several kinds of CPs with organic polymers to form mixed matrix membranes has recently offered a new possibility for Cu(I)-I nano-CPs. The combination of the mechanical properties displayed by the organic matrices plus the luminescent thermo/mechanochromism of the CPs opens the doors to the industrial fabrication of nano-sensors or smart packaging materials.

To sum up, we envision a great future for CPs based on Cu(I)-I chains, both in the fields of research and industry. Still, if we want these materials to be part of our every-day life, we must make an effort to dig deeper in their obtainment as nanostructures and their size-

dependent properties. These discoveries will surely have an impact on our society in a close future.

Acknowledgments

We thank financial support from the Spanish Ministerio de Economía y Competitividad (MINECO), MAT2016-77608-C3-1-P, MAT2016-75883-C2-2-P, MAT2016-75586-C4-4-P. JCE acknowledges the financial support by the "FPI-MINECO" Program of MINECO (Grant BES-2015-071534). This work is dedicated to Professors Francisco Urbanos and Reyes Jiménez.

References

[1] X.J. Loh, T.-C. Lee, Q. Dou, G.R. Deen, Biomater. Sci., 4 (2016) 70-86.

[2] I.T. Ahmed, A.A.A. Boraei, Spectr. Lett., 38 (2005) 47-59.

[3] D. Sheberla, L. Sun, M.A. Blood-Forsythe, S. Er, C.R. Wade, C.K. Brozek, A. Aspuru-Guzik, M. Dincă, J. Am. Chem. Soc., 136 (2014) 8859-8862.

[4] B. Zornoza, C. Tellez, J. Coronas, J. Gascon, F. Kapteijn, Micropor. Mesopor. Mater., 166 (2013) 67-78.

[5] Z. Zhang, Y. Zhao, Q. Gong, Z. Li, J. Li, Chem. Commun., 49 (2013) 653-661.

[6] C.M. Doherty, E. Knystautas, D. Buso, L. Villanova, K. Konstas, A.J. Hill, M. Takahashi, P. Falcaro, J. Mater. Chem., 22 (2012) 11470-11474.

[7] N. Armaroli, G. Accorsi, F. Cardinali, A. Listorti, Topics in Current Chemistry, 280 (2007) 69.

[8] T. Lebhardt, S. Roesler, M. Beck-Broichsitter, T. Kissel, J. Drug Deliv. Sci. Technol., 20 (2010) 171-180.

[9] J. Troyano, J. Perles, P. Amo-Ochoa, F. Zamora, S. Delgado, CrystEngComm, 18 (2016) 1809-1817.

[10] P. Zhou, R. Shi, J.-f. Yao, C.-f. Sheng, H. Li, Coord. Chem. Rev., 292 (2015) 107-143.

[11] R.A. Festa, D.J. Thiele, Curr. Biol., 21 (2011) R877-R883.

[12] S.V.S. Rana, J. Trace Elem. Med. Biol., 22 (2008) 262-284.

[13] A. Semisch, J. Ohle, B. Witt, A. Hartwig, Part. Fibre Toxicol., 11 (2014) 1-16.

[14] Y. Song, R.Q. Fan, P. Wang, X.M. Wang, S. Gao, X. Du, Y.L. Yang, T.Z. Luan, J. Mater. Chem. C, 3 (2015) 6249-6259.

[15] C. Slabbert, M. Rademeyer, Coord. Chem. Rev., 288 (2015) 18-49.

[16] S. Maderlehner, M.J. Leitl, H. Yersin, A. Pfitzner, Dalton Trans., 44 (2015) 19305-19313.

[17] J. Wang, ChemPhysChem, 10 (2009) 1748-1755.

[18] A. Hartwig, Free Radic. Biol. Med., 55 (2013) 63-72.

[19] K. Hassanein, P. Amo-Ochoa, C.J. Gomez-Garcia, S. Delgado, O. Castillo, P. Ocon, J.I. Martinez, J. Perles, F. Zamora, Inorg. Chem., 54 (2015) 10738-10747.

[20] Q. Benito, X.F. Le Goff, G. Nocton, A. Fargues, A. Garcia, A. Berhault, S. Kahlal, J.Y. Saillard, C. Martineau, J. Trebosc, T. Gacoin, J.P. Boilot, S. Perruchas, Inorg. Chem., 54 (2015) 4483-4494.

[21] P. Amo-Ochoa, K. Hassanein, C.J. Gomez-Garcia, S. Benmansour, J. Perles, O. Castillo, J.I. Martinez, P. Ocon, F. Zamora, Chem. Commun., 51 (2015) 14306-14309.

[22] N. Kitada, T. Ishida, CrystEngComm, 16 (2014) 8035-8040.

[23] Q. Benito, X.F. Le Goff, S. Maron, A. Fargues, A. Garcia, C. Martineau, F. Taulelle, S. Kahlal, T. Gacoin, J.P. Boilot, S. Perruchas, J. Am. Chem. Soc., 136 (2014) 11311-11320.

[24] W.-W. Zhou, W. Zhao, X. Zhao, F.-W. Wang, B. Wei, Synth. React. Inorg. Met.-Org. Nano-Met. Chem., 43 (2013) 1171-1174.

[25] J. Liu, Y.-L. Qin, M. Qu, R. Clerac, X.-M. Zhang, Dalton Trans., 42 (2013) 11571-11575.

[26] V.W.-W. Yam, K.M.-C. Wong, Chem. Commun., 47 (2011) 11579-11592.

[27] D. Braga, F. Grepioni, L. Maini, P.P. Mazzeo, B. Ventura, New J. Chem., 35 (2011) 339-344.

[28] R. Peng, M. Li, D. Li, Coord. Chem. Rev., 254 (2010) 1-18.

[29] F. Wu, H. Tong, K. Wang, J. Zhang, Z. Xu, X. Zhu, Inorg. Chem. Commun., 58 (2015) 113-116.

[30] S.-M. Fang, Q. Zhang, M. Hu, B. Xiao, L.-M. Zhou, G.-H. Sun, L.-J. Gao, M. Du, C.-S. Liu, CrystEngComm, 12 (2010) 2203-2212.

[31] T.H. Kim, Y.W. Shin, J.S. Kim, S.S. Lee, J. Kim, Inorg. Chem. Commun., 10 (2007) 717-719.

[32] J.-C. Li, H.-X. Li, H.-Y. Li, W.-J. Gong, J.-P. Lang, Cryst. Growth Des., 16 (2016) 1617-1625.

[33] P. Lin, R.A. Henderson, R.W. Harrington, W. Clegg, C.-D. Wu, X.-T. Wu, Inorg. Chem., 43 (2003) 181-188.

[34] J.H. Yu, J.Q. Xu, L. Ye, H. Ding, W.J. Jing, T.G. Wang, J.N. Xu, H.B. Jia, Z.C. Mu, G.D. Yang, Inorg. Chem. Commun., 5 (2002) 572-576.

[35] H.D. Hardt, A. Pierre, Z. Anorg. Allg. Chem., 402 (1973) 107-112.

[36] H.-B. Zhu, L. Liang, J. Coord. Chem., 68 (2015) 1306-1316.

[37] A.D. Khalaji, K. Jafari, B. Bahramian, K. Fejfarova, M. Dusek, Monatsh. Chem., 144 (2013) 1621-1626.

[38] S.-L. Li, R. Zhang, J.-J. Hou, X.-M. Zhang, Inorg. Chem. Commun., 32 (2013) 12-17.

[39] H.-B. Zhu, W.-N. Yang, R.-Y. Shan, J. Coord. Chem., 66 (2013) 435-443.

[40] L.-M. Wan, Z. Yang, A.-X. Zheng, Z.-G. Ren, J.-P. Lang, Acta. Crystallogr. Sect. C, 68 (2012) M181-M184.

[41] D. Prochowicz, I. Justyniak, A. Kornowicz, T. Kaczorowski, Z. Kaszkur, J. Lewinski, Chem. Eur. J., 18 (2012) 7367-7371.

[42] J.P. Safko, J.E. Kuperstock, S.M. McCullough, A.M. Noviello, X. Li, J.P. Killarney, C. Murphy, H.H. Patterson, C.A. Bayse, R.D. Pike, Dalton Trans., 41 (2012) 11663-11674.

[43] Q. Hou, X.-J. Qu, J. Jin, J.-J. Zhao, J.-H. Yu, J.-Q. Xu, J. Cluster Sci., 22 (2011) 715-722.

[44] Y.-J. Fan, J.-Y. Liu, S.-Q. Zang, Y. Zhou, H.-W. Hou, J. Inorg. Organomet. P., 21 (2011) 718-722.

[45] L. Li, Z. Ren, X. Lue, H. Wang, Y. Chang, H. Li, B. Wu, J. Lang, Sci. China Chem., 53 (2010) 2083-2090.

[46] S. Hu, F.-Y. Yu, Y. Yan, Z.-F. Hao, L. Yu, M.-L. Tong, Inorg. Chem. Commun., 14 (2011) 622-625.

[47] Z.-M. Hao, J. Wang, X.-M. Zhang, CrystEngComm, 12 (2010) 1103-1109.

[48] K. Tsuge, Y. Chishina, H. Hashiguchi, Y. Sasaki, M. Kato, S. Ishizaka, N. Kitamura, Coord. Chem. Rev., 306, Part 2 (2016) 636-651.

[49] E. Cariati, E. Lucenti, C. Botta, U. Giovanella, D. Marinotto, S. Righetto, Coord. Chem. Rev., 306, Part 2 (2016) 566-614.

[50] E. Cariati, J. Bourassa, Chem. Commun., (1998) 1623-1624.

[51] E. Cariati, X. Bu, P.C. Ford, Chem. Mater., 12 (2000) 3385-3391.

[52] P.C. Ford, E. Cariati, J. Bourassa, Chem. Rev., 99 (1999) 3625-3648.

[53] O.S. Wenger, Chem. Rev., 113 (2013) 3686-3733.

[54] R.-Y. Wang, X. Zhang, Q.-F. Yang, Q.-S. Huo, J.-H. Yu, J.-N. Xu, J.-Q. Xu, J. Solid State Chem., 251 (2017) 176-185.

[55] Y. Chen, Z.-O. Wang, Z.-G. Ren, H.-X. Li, D.-X. Li, D. Liu, Y. Zhang, J.-P. Lang, Cryst. Growth Des., 9 (2009) 4963-4968.

[56] G. Givaja, P. Amo-Ochoa, C.J. Gomez-Garcia, F. Zamora, Chem. Soc. Rev., 41 (2012) 115-147.

[57] X.-W. Lei, C.-Y. Yue, J.-Q. Zhao, Y.-F. Han, J.-T. Yang, R.-R. Meng, C.-S. Gao, H. Ding, C.-Y. Wang, W.-D. Chen, Cryst. Growth Des., 15 (2015) 5416-5426.

[58] J. Liu, Y.-H. Tang, F. Wang, J. Zhang, CrystEngComm, 20 (2018) 1232-1236.

[59] J.P. Killarney, M. McKinnon, C. Murphy, K.M. Henline, C. Wang, R.D. Pike, H.H. Patterson, Inorg. Chem. Commun., 40 (2014) 18-21.

[60] F. Wang, Y.-T. Wang, H. Yu, J.-X. Chen, B.-B. Gao, J.-P. Lang, Inorg. Chem., 55 (2016) 9417-9423.

[61] S. Bouson, A. Krittayavathananon, N. Phattharasupakun, P. Siwayaprahm, M. Sawangphruk, R. Soc. Open Sci., 4 (2017).

[62] R. Toivola, P.-N. Lai, J. Yang, S.-H. Jang, A.K.Y. Jen, B.D. Flinn, Compos. Sci. Technol., 139 (2017) 74-82.

[63] Z.a. Li, R. Toivola, F. Ding, J. Yang, P.-N. Lai, T. Howie, G. Georgeson, S.-H. Jang, X. Li, B.D. Flinn, A.K.-Y. Jen, Adv. Mater., 28 (2016) 6592-6597.

[64] K. Hassanein, J. Conesa-Egea, S. Delgado, O. Castillo, S. Benmansour, J.I. Martínez, G. Abellán, C.J. Gómez-García, F. Zamora, P. Amo-Ochoa, Chem. Eur. J., 21 (2015) 17282-17292.

[65] J. Conesa-Egea, J. Gallardo-Martínez, S. Delgado, J.I. Martínez, J. Gonzalez-Platas, V. Fernández-Moreira, U.R. Rodríguez-Mendoza, P. Ocón, F. Zamora, P. Amo-Ochoa, Small, 13 (2017), 1700965.

[66] W. Liu, Y. Fang, G.Z. Wei, S.J. Teat, K. Xiong, Z. Hu, W.P. Lustig, J. Li, J. Am. Chem. Soc., 137 (2015) 9400-9408.

[67] Y. Song, R. Fan, P. Wang, X. Wang, S. Gao, X. Du, Y. Yang, T. Luan, J. Mater. Chem. C, 3 (2015) 6249-6259.

[68] K. Singh, J.R. Long, P. Stavropoulos, J. Am. Chem. Soc., 119 (1997) 2942-2943.

[69] U. Siemeling, U. Vorfeld, B. Neumann, H.-G. Stammler, Chem. Commun., (1997) 1723-1724.

[70] H.D. Hardt, A. Pierre, Inorg. Chim. Acta, 25 (1977) L59-L60.

[71] Z. Liu, P.I. Djurovich, M.T. Whited, M.E. Thompson, Inorg. Chem., 51 (2012) 230-236.

[72] W. Liu, Y. Fang, G.Z. Wei, S.J. Teat, K. Xiong, Z. Hu, W.P. Lustig, J. Li, J. Am. Chem. Soc., 137 (2015) 9400-9408.

[73] X.-c. Shan, F.-l. Jiang, D.-q. Yuan, H.-b. Zhang, M.-y. Wu, L. Chen, J. Wei, S.-q. Zhang, J. Pan, M.-c. Hong, Chem. Sci., 4 (2013) 1484-1489.

[74] J. Conesa-Egea, N. Nogal, J.I. Martínez, V. Fernández-Moreira, U.R. Rodríguez-Mendoza, J. González-Platas, C.J. Gómez-García, S. Delgado, F. Zamora, P. Amo-Ochoa, Chem. Sci., in press (2018). https://doi.org/10.1039/c8sc03085e.

[75] J. Pospisil, I. Jess, C. Näther, M. Necas, P. Taborsky, New J. Chem., 35 (2011) 861-864.

[76] J.-Y. Niu, M.-X. Li, J.-P. Wang, Y. Bo, J. Chem. Crystallogr., 33 (2003) 799-803.

[77] I. Jeß, P. Taborsky, J. Pospíšil, C. Näther, Dalton Trans., (2007) 2263-2270.

[78] C. Näther, I. Jeß, Monatsh. Chem., 132 (2001) 897-910.

[79] E. Redel, M. Fiederle, C. Janiak, Z. Anorg. Allg. Chem., 635 (2009) 1139-1147.

[80] E. Mateo-Marti, L. Welte, P. Amo-Ochoa, P.J. Sanz Miguel, J. Gomez-Herrero, J.A. Martin-Gago, F. Zamora, Chem. Commun., (2008) 945-947.

[81] A. Vogler, H. Kunkely, J. Am. Chem. Soc., 108 (1986) 7211-7212.

[82] D. Tran, J.L. Bourassa, P.C. Ford, Inorg. Chem., 36 (1997) 439-442.

[83] Q. Benito, B. Baptiste, A. Polian, L. Delbes, L. Martinelli, T. Gacoin, J.-P. Boilot, S. Perruchas, Inorg. Chem., 54 (2015) 9821-9825.

[84] A. Aguirrechu-Comeron, R. Hernandez-Molina, P. Rodriguez-Hernandez, A. Munoz, U.R. Rodriguez-Mendoza, V. Lavin, R.J. Angel, J. Gonzalez-Platas, Inorg. Chem., 55 (2016) 7476-7484.

[85] C.L. Raston, A.H. White, J. Chem. Soc. Dalton Trans., (1976) 2153-2156.

[86] E. Eitel, D. Oelkrug, Z. Naturforsch. 35B (1980) 1247-1253.

[87] R. P. Feynman, There's Plenty of Room at the Bottom. http://www.zyvex.com/nanotech/feynman.html, 1959. (access Aug. 27 2018).

[88] C.J. Chen, An Introduction to Scanning Tunneling Microscopy, second ed., Oxford University Press, Oxford, 2008.

[89] P. Hansma, V. Elings, O. Marti, C. Bracker, Science, 242 (1988) 209-216.

[90] T. Schwerdtle, A. Hartwig, Mat.-wiss. u. Werkstofftech., 37 (2006) 521-525.

[91] Y. Yamamoto, T. Miura, M. Suzuki, N. Kawamura, H. Miyagawa, T. Nakamura, K. Kobayashi, T. Teranishi, H. Hori, Phys. Rev. Lett., 93 (2004) 116801.

[92] Y. Qiao, Y. Lin, Y. Wang, Z. Yang, J. Liu, J. Zhou, Y. Yan, J. Huang, Nano Lett., 9 (2009) 4500-4504.

[93] J. Xiong, Y.J. Lan, S.F. Zhang, Russ. J. Coord. Chem., 33 (2007) 306-311.

[94] P. Scharf, J. Muller, ChemPlusChem, 78 (2013) 20-34.

[95] M.S. Deshmukh, A. Yadav, R. Pant, R. Boomishankar, Inorg Chem, 54 (2015) 1337-1345.

[96] C. Neaime, C. Daiguebonne, G. Calvez, S. Freslon, K. Bernot, F. Grasset, S. Cordier, O. Guillou, Chem. Eur. J., 21 (2015) 17466-17473.

[97] K.A. Brown, X. Yang, D. Schipper, J.W. Hall, L.J. DePue, A.J. Gnanam, J.F. Arambula, J.N. Jones, J. Swaminathan, Y. Dieye, J. Vadivelu, D.J. Chandler, E.M. Marcotte, J.L. Sessler, L.I.R. Ehrlich, R.A. Jones, Dalton Trans., 44 (2015) 2667-2675.

[98] K. Baek, G. Yun, Y. Kim, D. Kim, R. Hota, I. Hwang, D. Xu, Y.H. Ko, G.H. Gu, J.H. Suh, C.G. Park, B.J. Sung, K. Kim, J. Am. Chem. Soc., 135 (2013) 6523-6528.

[99] S. Awakumova, P. Verderio, G. Speranza, F. Porta, J. Phys. Chem. C, 117 (2013) 3002-3010.

[100] O.S. Wolfheis, Angew. Chem. Int. Ed., 48 (2009) 2268-2269.

[101] R.E. Morris, P.S. Wheatley, Angew. Chem. Int. Ed., 47 (2008) 4966-4981.

[102] A. Semisch, A. Hartwig, Chem. Res. Toxicol., 27 (2014) 169-171.

[103] J. Zhao, Y.-N. Wang, W.-W. Dong, Y.-P. Wu, D.-S. Li, Q.-C. Zhang, Inorg. Chem., 55 (2016) 3265-3271.

[104] D. Rodriguez-San-Miguel, P. Amo-Ochoa, F. Zamora, Chem. Commun., 52 (2016) 4113-4127.

[105] P. Amo-Ochoa, L. Welte, R. Gonzalez-Prieto, P.J. Sanz Miguel, C.J. Gomez-Garcia, E. Mateo-Marti, S. Delgado, J. Gomez-Herrero, F. Zamora, Chem. Commun., 46 (2010) 3262-3264.

[106] A. Guijarro, O. Castillo, L. Welte, A. Calzolari, P. J. Sanz Miguel, C. J. Gómez-García, D. Olea, R. di Felice, J. Gómez-Herrero, F. Zamora, Adv. Funct. Mater., 20 (2010) 1451-1457.

[107] D. Olea, R. González-Prieto, J. L. Priego, M. C. Barral, P. J. de Pablo, M. R. Torres, J. Gómez-Herrero, R. Jiménez-Aparicio, F. Zamora, Chem. Commun., (2007) 1591-1593.

[108] L. Welte, R. González-Prieto, D. Olea, M. R. Torres, J. L. Priego, R. Jiménez-Aparicio, J. Gómez-Herrero, F. Zamora, ACS Nano, 2 (2008) 2051-2056.

[109] J. Troyano, J. Perles, P. Amo-Ochoa, J.I. Martínez, F. Zamora, S. Delgado, CrystEngComm., 16 (2014) 8224-8231.

[110] J. Conesa-Egea, K. Hassanein, M. Muñoz, F. Zamora, P. Amo-Ochoa, Dalton Trans., 47 (2018) 5607-5613.

[111] J. Conesa-Egea, C.D. Redondo, J. Ignacio Martinez, C.J. Gomez-Garcia, O. Castillo, F. Zamora, P. Amo-Ochoa, Inorg. Chem., 57 (2018) 7568-7577.

[112] T. Rodenas, I. Luz, G. Prieto, B. Seoane, H. Miro, A. Corma, F. Kapteijn, F. X. Llabrés i Xamena, J. Gascon, Nat. Mater., 14 (2015) 48-55.

[113] M.S. Denny, S.M. Cohen, Angew. Chem. Int. Ed., 54 (2015) 9029-9032.

[114] W. Chen, R. Fan, H. Zhang, Y. Dong, P. Wang, Y. Yang, Dalton Trans., 46 (2017) 4265-4277.

[115] J. Troyano, O. Castillo, J.I. Martínez, V. Fernández-Moreira, Y. Ballesteros, D. Maspoch, F. Zamora, S. Delgado, Adv. Funct. Mater., 28 (2018) 1704040.